The Astrophysical Journal, 868:58 (7pp), 2018 November 20 https://doi.org/10.3847/1538-4357/aae6c4

An Intrinsic Link between Long-term UV/Optical Variations and X-Ray Loudness in Quasars

Wen-yong Kang[1,2], Jun-Xian Wang[1,2], Zhen-Yi Cai[1,2], Heng-Xiao Guo[3], Fei-Fan Zhu[1,2], Xin-Wu Cao[4,6,7], Wei-Min Gu[5,7], and Feng Yuan[4,7]

[1] CAS Key Laboratory for Researches in Galaxies and Cosmology, University of Science and Technology of China, Chinese Academy of Sciences, Hefei, Anhui 230026, People's Republic of China; kwy0719@mail.ustc.edu.cn, jxw@ustc.edu.cn, zcai@ustc.edu.cn
[2] School of Astronomy and Space Science, University of Science and Technology of China, Hefei 230026, People's Republic of China
[3] Department of Astronomy, University of Illinois at Urbana-Champaign, Urbana, IL 61801, USA
[4] Shanghai Astronomical Observatory, Chinese Academy of Sciences, 80 Nandan Road, Shanghai 200030, People's Republic of China
[5] Department of Astronomy, Xiamen University, Xiamen, Fujian 361005, People's Republic of China
[6] Key Laboratory of Radio Astronomy, Chinese Academy of Sciences, Nanjing 210008, People's Republic of China
[7] SHAO-XMU Joint Center for Astrophysics, Xiamen University, Xiamen, Fujian 361005, People's Republic of China
Received 2018 July 30; revised 2018 September 25; accepted 2018 October 6; published 2018 November 20

Abstract

Observations have shown that the UV/optical variation amplitude of quasars depends on several physical parameters including luminosity, Eddington ratio, and possibly black hole mass. Identifying new factors which correlate with the variation is essential to probing the underlying physical processes. Combining around 10 years of quasar light curves from SDSS stripe 82 and X-ray data from Stripe 82X, we build a sample of X-ray-detected quasars to investigate the relation between UV/optical variation amplitude ($\sigma_{\rm rms}$) and X-ray loudness. We find that quasars with more intense X-ray radiation (compared to bolometric luminosity) are more variable in the UV/optical. This correlation remains highly significant after excluding the effect of other parameters including luminosity, black hole mass, Eddington ratio, redshift, and rest frame wavelength (i.e., through partial correlation analyses). We further find that the intrinsic link between X-ray loudness and UV/optical variation is gradually more prominent on longer timescales (up to 10 yr in the observed frame), but tends to disappear at timescales $<$100 days. This suggests a slow and long-term underlying physical process. The X-ray reprocessing paradigm, in which the UV/optical variation is produced by variable central X-ray emission illuminating the accretion disk, is thus disfavored. This discovery points to an interesting scenario in which both the X-ray coronal heating and UV/optical variation in quasars are closely associated with magnetic disc turbulence, and the innermost disc turbulence (where coronal heating occurs) correlates with slow turbulence at larger radii (where UV/optical emission is produced).

Key words: accretion, accretion disks – galaxies: active – quasars: general – X-rays: galaxies

1. Introduction

Active galactic nuclei (AGNs) and quasars, powered by central accreting supermassive black holes, show aperiodical variations from radio waves to X-rays and gamma-rays. Investigating the nature of such variations and the underlying physics is one of the main subjects of modern time-domain astronomy. In particular, studies on the variation of the UV/optical emission, predominantly produced in the accretion disk, are helpful in probing the underlying physics of the inner accretion process.

Observational studies have established clear (anti-)correlations between the UV/optical variation amplitude and several known parameters. UV/optical variability decreases with wavelength (e.g., Vanden Berk et al. 2004; Wilhite et al. 2005; Meusinger et al. 2011; Zuo et al. 2012), and luminosity, likely driven by the Eddington ratio (e.g., Vanden Berk et al. 2004; Wilhite et al. 2008; Ai et al. 2010; Zuo et al. 2012; Meusinger & Weiss 2013; Sun et al. 2018). The intrinsic correlation with black hole mass is less clear, after isolating the influence of luminosity or Eddington ratio, and rest frame wavelength (e.g., Wold et al. 2007; Wilhite et al. 2008; Bauer et al. 2009; MacLeod et al. 2010; Zuo et al. 2012; Meusinger & Weiss 2013; Kozłowski 2016). A weak positive correlation between the variation and redshift is also reported, after isolating the effects of rest frame wavelength and luminosity (Vanden Berk et al. 2004), but several other studies have claimed no significant cosmological evolution (e.g., MacLeod et al. 2010; Meusinger et al. 2011; Zuo et al. 2012).

Does the quasar variation correlate with additional observable parameters? It is interesting to note that at the aforementioned fixed physical parameters, quasars exhibit too large a scatter in their variation to be attributed to sparse light curve sampling and photometric uncertainties (MacLeod et al. 2012; Guo et al. 2017), suggesting that the variation correlates with additional unknown factors.

The characteristic timescales of quasar UV/optical variations were found to be consistent with the disk thermal timescale, and the variations can thus be attributed to thermal fluctuations in the disk, likely driven by a turbulent magnetic field (e.g., Kelly et al. 2009). In this scenario the variation amplitude is controlled by the strength of the turbulence. Identifying additional parameters which correlate with variation is thus essential to study the causes or effects of magnetic turbulence.

The central compact hot X-ray corona in AGNs is widely believed to be heated by magnetic reconnection in the innermost regions, which is directly associated with magnetic turbulence (e.g., Galeev et al. 1979; Di Matteo 1998). Searching for direct observational evidence for this scenario, however, is rather challenging. We speculate that there exists an observable link between X-ray radiation and UV/optical

variation, i.e., in quasars with stronger accretion disk turbulence (stronger UV/optical variation), coronal heating is more efficient (higher X-ray power).

SDSS Stripe 82, a 290 $\deg^2$ equatorial field of the sky, has been scanned around 60 times in the *ugriz* bands by the Sloan Digital Sky Survey (Sesar et al. 2007). MacLeod et al. (2012) presented recalibrated ∼10 yr long SDSS *ugriz* light curves for 9275 spectroscopically confirmed quasars in Stripe 82, for most of which measurements of black hole mass, absolutely magnitude (K-corrected), and bolometric luminosity are available from Shen et al. (2011). Stripe 82X, an X-ray survey using *Chandra* and *XMM-Newton* observations, covers 31.3 $\deg^2$, overlapping the Stripe 82 field (LaMassa et al. 2016; Ananna et al. 2017). A catalog of 6181 unique X-ray sources has been released (LaMassa et al. 2016), enabling us for the first time to explore the relation between X-ray emission and UV/optical variation in a large quasar sample.

In Section 2 we present the cross-matched quasar sample, along with the measurements of variation amplitude for these quasars. We perform correlation analyses in Section 3 to reveal the intrinsic correlation between UV/optical variation and X-ray loudness, and a positive and statistically robust correlation is reported. A discussion on this new discovery is given in Section 4. Throughout this work, cosmological parameters of $H_0 = 70\ \mathrm{km\ s^{-1}} \cdot \mathrm{Mpc^{-1}}$, $\Omega_m = 0.3$ and $\Omega_\Lambda = 0.7$ are adopted.

2. Quasar Sample

Shen et al. (2011) presented physical properties (including black hole mass M, bolometric luminosity $L_{\rm bol}$, and Eddington ratio $\dot{m}$) of 105,783 quasars in the SDSS DR7 quasar catalog. We cross-match those quasars with the optical counterparts of the Stripe 82X X-ray source catalog (Ananna et al. 2017), using a matching radius of 0.″7. A total of 679 unique matches are found.[8] We obtain their *ugri*-band light curves from MacLeod et al. (2012). We drop the z-band light curves whose photometric uncertainties are significantly larger and where the intrinsic variations of quasars are considerably weaker compared with the other four bands. Light curve data points with photometric uncertainties >0.2 mag (∼0.9% of all data points), mostly due to poor observing conditions, are also dropped. To ensure accurate measurement of the variation amplitudes with the sparsely sampled light curves, we only include quasars with at least 20 photometric data points in each of the light curves. We further exclude quasars with redshift >1.9 from this study, for which the black hole mass derived from the CIV line could be significantly biased (e.g., Coatman et al. 2016, 2017). The final sample contains 499 quasars, with soft (0.5–2 keV), hard (2.0–10.0 keV), and total (0.5–10.0 keV) band X-ray fluxes available for 492, 360, and all of them, respectively.

For each quasar, the intrinsic variation amplitude in each band is measured with the excess variance $\sigma_{\rm rms}$ (Vaughan et al. 2003; see also Sesar et al. 2007; Zuo et al. 2012)

$$\sigma^2_{\rm rms} = \frac{1}{N-1}\sum (X_i - \bar{X})^2 - \frac{1}{N}\sum \sigma_i^2 \qquad (1)$$

where N is the number of photometric measurements, X_i the observed magnitude, $\bar{X}$ the average magnitude, and σ_i the photometric uncertainty of each observation. In case of no intrinsic variation, the expected value of $\sigma^2_{\rm rms}$ is zero, with a statistical uncertainty of

$$\mathrm{err}(\sigma^2_{\rm rms}) = \sqrt{\frac{2}{N}} \times \frac{1}{N}\sum \sigma_i^2 \qquad (2)$$

due to photometric errors (Vaughan et al. 2003). In the following analysis, we assign a 2σ upper limit to $\sigma^2_{\rm rms}$ for sources with $\sigma^2_{\rm rms}/\mathrm{err}(\sigma^2_{\rm rms}) < 2$.

We note that many studies model quasar light curves with the damped random walk process (Kelly et al. 2009; Kozłowski et al. 2010; MacLeod et al. 2010; Zu et al. 2013), with two model parameters: τ (the characteristic timescale) and SF_∞ (structure function). However, these parameters can be poorly constrained with SDSS Stripe 82 light curves (due to the limited length and the sparse sampling; e.g., Kozłowski 2017). In this work we simply adopt the standard $\sigma_{\rm rms}$, which describes the variation with a single parameter, to measure the ∼10 yr long variation amplitude of each quasar and study its correlation with other parameters.

3. Correlation Analyses

We adopt the ratio of X-ray luminosity to bolometric luminosity to represent the relative strength of X-ray emission in each quasar, which we call X-ray loudness, and investigate its correlation with UV/optical variation amplitude through simple linear regression:

$$\sigma_{\rm rms} \sim (L_{\rm X}/L_{\rm bol})^{s_0}. \qquad (3)$$

In Figure 1 we plot *ugri* $\sigma_{\rm rms}$ versus $L_{0.5-10keV}/L_{\rm bol}$, where clear positive correlations are seen. Note that here we present X-ray loudness based on 0.5–10 keV band X-ray luminosity. Using soft and hard X-ray bands yields similar results. Along with the best-fit linear regression slope s, in Figure 1 we also present the Spearman's rank correlation coefficient and the corresponding significance level (r and rcc). Note that the Spearman's rank correlation is a non-parametric approach with no prior assumption on either the data distribution or the form of the relationship between two quantities. Clearly, both approaches (linear regression and Spearman's rank) yield clear positive correlations between $\sigma_{\rm rms}$ and X-ray loudness, though with considerable scatter (∼0.2 dex along the vertical axis; see Figure 1).

Such correlations demonstrate that sources with relatively stronger X-ray emission tend to be more variable in the UV/optical. However, a solid link between them cannot yet be established as it is known that both X-ray loudness and UV/optical variation anticorrelate with luminosity (or Eddington ratio) (Bauer et al. 2009; Lusso et al. 2010, 2012; Meusinger et al. 2011; Zuo et al. 2012; Fanali et al. 2013; Meusinger & Weiss 2013); thus the correlations we plot in Figure 1 might be just secondary effects. We perform linear regression to examine whether X-ray loudness and UV/optical variation in our sample correlate with common physical parameters including black hole mass M, Eddington ratio $\dot{m}$, redshift z, and $L_{\rm bol}$ (Figure 2). We see that in our sample both $\sigma_{\rm rms}$ and X-ray loudness significantly and similarly anticorrelate with $L_{\rm bol}$, and $\dot{m}$, and marginally anticorrelate with redshift. Meanwhile there

[8] There are 15 quasars which are associated with two X-ray sources, for which we choose the X-ray counterpart closest to the optical position.

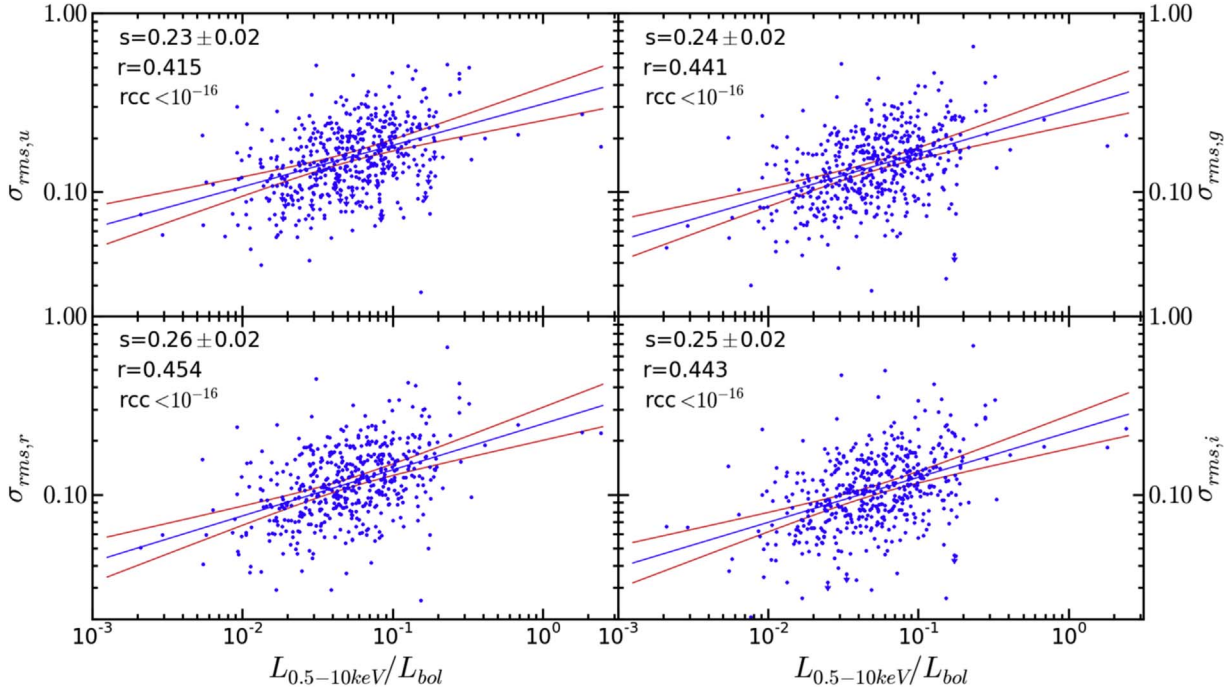

Figure 1. Variation amplitude $\sigma_{\rm rms}$ (in units of magnitude) in the SDSS *ugri* bands vs. X-ray loudness for quasars in SDSS Stripe 82. Blue lines plot the best-fit correlations (through simple linear regression) with 3σ confidence bands (red lines). The best-fit linear regression slope s, the Spearman's rank correlation coefficient, and the significance level (r and rcc) are given in the upper left corner in each panel.

is no apparent correlation between $\sigma_{\rm rms}$ and M, and a marginal negative correlation between X-ray loudness and M.[9]

Partial correlation analyses were thus required to investigate whether there is an intrinsic correlation between UV/optical variation and X-ray loudness, by controlling the effect of $\dot{m}$, M, and redshift. Note that as $\dot{m}$ is the ratio of $L_{\rm bol}$ and M, the effect of $L_{\rm bol}$ is also simultaneously controlled during the analyses. Replacing $\dot{m}$ with $L_{\rm bol}$ during the analyses does not alter the results. The correlation coefficient and the significance level (r and rcc) are shown in Table 1, and the intrinsic correlations are weaker than the apparent ones (Figure 1), but remain statistically significant. Such positive intrinsic correlations show that, for two quasars with the same bolometric luminosity, black hole mass, and redshift, the one with higher X-ray loudness is more variable in the UV/optical.

Multiple linear regression analyses were then run to quantify the relations between UV/optical variation and physical parameters including Eddington ratio, black hole mass, redshift, and X-ray loudness:

$$\sigma_{\rm rms} \sim \dot{m}^a M^b (1+z)^c (L_{\rm X}/L_{\rm bol})^s \quad (4)$$

and the best-fit parameters are also given in Table 1, indicating a clear intrinsic correlation between $\sigma_{\rm rms}$ and $L_{\rm X}/L_{\rm bol}$. Again, replacing $\dot{m}$ with $L_{\rm bol}$ in the equation would not alter the main results presented in this work.

To illustrate the intrinsic correlation between $\sigma_{\rm rms}$ and $L_X/L_{\rm bol}$ obtained in Equation (4), we plot in Figure 3 the correlations between the residuals of Equation (5) and those of Equation (6):

$$\sigma_{\rm rms} \sim \dot{m}^{a1} M^{b1} (1+z)^{c1} \quad (5)$$

$$L_{\rm X}/L_{\rm Edd} \sim \dot{m}^{a2} M^{b2} (1+z)^{c2}. \quad (6)$$

In Figure 3 the scatter is similar to that in Figure 1. This scatter could be due to X-ray flux variation, sparse SDSS photometric sampling in Stripe 82, red noise leakage (Guo et al. 2017), uncertainties in M and $L_{\rm bol}$ measurements, or other unknown parameters which either X-ray loudness or $\sigma_{\rm rms}$ might rely on.

The partial correlation analyses above demonstrate positive intrinsic correlations between single-band $\sigma_{\rm rms}$ (u, g, r, i) and X-ray loudness. We note that a single SDSS band observes different rest frame wavelengths for sources at various redshifts. The $\sigma_{\rm rms}$ from the four bands can be analyzed jointly by assigning a rest frame wavelength λ_c to each measurement of $\sigma_{\rm rms}$ (the central wavelength of the corresponding SDSS band divided by $1+z$). We then perform partial correlation analyses between $\sigma_{\rm rms}$ (λ_c) and X-ray loudness, controlling the effect of bolometric luminosity, black hole mass (thus also Eddington ratio), redshift, and rest frame wavelength. The resulting partial correlation coefficients are presented in Table 1, which also shows a statistically significant intrinsic correlation between $\sigma_{\rm rms}$ and X-ray loudness. We then run a multiple linear regression to quantify the correlations:

$$\sigma_{\rm rms} \sim \dot{m}^a (M_{\rm BH})^b (1+z)^c \lambda_{\rm RF}^d (L_{\rm X}/L_{\rm bol})^s \quad (7)$$

and the derived best-fit slopes are presented in Table 1. We note, however, that caution is needed regarding the significance levels of the partial correlation in the joint analysis, as the four band $\sigma_{\rm rms}$ measurements of a single quasar are not completely independent of each other.

4. Discussion

Using SDSS light curves from Stripe 82 and X-ray detections from Stripe 82X, we for the first time examine the correlation between the UV/optical variation amplitude and

[9] However, revealing the intrinsic correlation with M requires isolating the influence of luminosity/Eddington ratio and redshift, which is beyond the scope of this work.

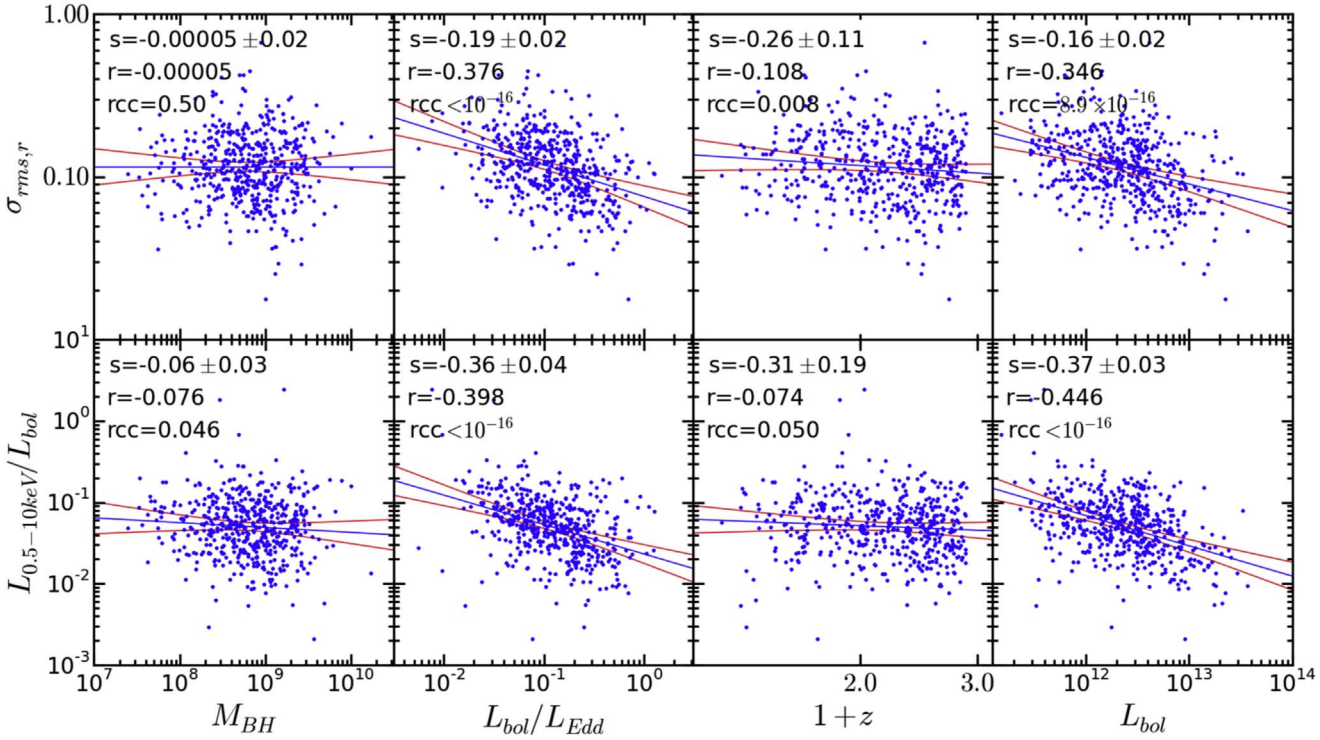

Figure 2. Correlation between $\sigma_{\rm rms}$ (upper panels), X-ray loudness (lower panels), and black hole mass, Eddington ratio, redshift, and bolometric luminosity. Symbols and lines are the same as in Figure 1.

X-ray loudness of quasars. Partial correlation analyses reveal a robust intrinsic correlation between them, controlling the effects of other fundamental physical parameters including bolometric luminosity, black hole mass, Eddington ratio, redshift, and rest frame wavelength. Such intrinsic correlation indicates for quasars with identical $L_{\rm bol}$, M, $\dot{m}$ and z, the ones with stronger UV/optical variations at identical rest wavelength are X-ray louder, or vice versa.

4.1. Robustness of the Intrinsic Correlation between UV/Optical Variation and X-Ray Loudness

We note that our sample is limited to SDSS quasars with Stripe 82X X-ray detections. Stripe 82X covers an area of 31.3 deg^2, while S82 covers an area of 290 deg^2. Taking the sky coverages into consideration, we estimate an X-ray completeness of ∼73% for our sample (of all $z < 1.9$ SDSS quasars with M and $L_{\rm bol}$ measurements and sufficient light curve data points in Stripe 82X).[10] Would the sample incompleteness in X-rays produce an artificial correlation between $\sigma_{\rm rms}$ and X-ray loudness? We perform simulations to address this issue. Equation (5) measures the dependency of $\sigma_{\rm rms}$ (X-ray loudness) on Eddington ratio, mass, and redshift, and similarly Equation (6) measures the dependency of X-ray loudness against these parameters.

For each individual quasar, starting from its Eddington ratio, mass, and redshift, we calculate its expected $\sigma_{\rm rms}$ and X-ray loudness based on the best-fit correlations in Equations (5) and (6). We then add random Gaussian fluctuations (with variance derived from the residuals of Equations (5) and (6)) to the expected $\sigma_{\rm rms}$ and X-ray loudness. Obviously the simulated $\sigma_{\rm rms}$ and X-ray loudness show no intrinsic correlation at all (controlling the effects of observed Eddington ratio, mass, and redshift), and this is confirmed using partial correlation and multiple linear regression analyses. We then apply an X-ray flux cut to this simulated sample to mimic the effect of an X-ray incomplete sample. The cut is selected to exclude 27% of the X-ray weak sources in the sample. The resulting incomplete sample does not show any "intrinsic" correlation between $\sigma_{\rm rms}$ and X-ray loudness.

It is known that the measurements of black hole mass and bolometric luminosity of quasars are prone to considerable uncertainties. Assuming both $\sigma_{\rm rms}$ and X-ray loudness correlate with luminosity or Eddington ratio, but do not have an intrinsic correlation with each other, the uncertainties in M and $L_{\rm bol}$ might lead to an artificial partial correlation between $\sigma_{\rm rms}$ and X-ray loudness. We perform Monte Carlo simulations to address this effect. Again, from Equations (5) and (6) we build artificial samples with no intrinsic correlation between the simulated $\sigma_{\rm rms}$ and X-ray loudness. We then add random fluctuations to the observed $L_{\rm bol}$ and M for each quasar. For mass measurement, we adopt a conservative 0.4 dex calibration uncertainty (Shen et al. 2011), and add it quadratically to the direct measurement error from Shen et al. (2011). For $L_{\rm bol}$, both a 0.08 dex uncertainty (20%, to take care of the uncertainty in the bolometric correction; Richards et al. 2006) and a direct measurement error from Shen et al. (2011) are included. No fluctuation is added to redshift as it has a very small uncertainty. Partial correlation analyses using the simulated $\sigma_{\rm rms}$, X-ray loudness, $L_{\rm bol}$, and M, however, do not yield a significant intrinsic correlation between $\sigma_{\rm rms}$ and X-ray loudness. We conclude that the observed correlation between $\sigma_{\rm rms}$ and X-ray loudness is physical, and cannot be attributed to any observational effect.

[10] In the full 290 deg^2 S82 area, there are 6306 $z < 1.9$ quasars with M and $L_{\rm bol}$ measurements and at least 20 data points in each light curve. We expect ∼680 such quasars in the 31.3 deg^2 S82X area, and our final sample consists of 499 quasars with full X-ray-band detection.

Table 1
Partial Correlation Coefficients and Multiple Linear Regression Slopes between $\sigma_{\rm rms}$ and Other Physical Parameters

$\sigma_{\rm rms}$	r	rcc	$\dot{m}$ (a)	M (b)	1+z (c)	λ_c (d)	$L_{\rm X}/L_{\rm bol}$ (s)	X-Ray band
u	0.230	1.4×10^{-7}	-0.20 ± 0.03	-0.09 ± 0.03	0.15 ± 0.14		0.13 ± 0.02	
g	0.276	2.5×10^{-10}	-0.18 ± 0.03	-0.06 ± 0.03	0.28 ± 0.14		0.16 ± 0.02	
r	0.283	8.7×10^{-11}	-0.18 ± 0.03	-0.07 ± 0.03	0.11 ± 0.14		0.17 ± 0.02	soft
i	0.290	3.2×10^{-11}	-0.16 ± 0.03	-0.05 ± 0.03	-0.06 ± 0.14		0.17 ± 0.02	
$u+g+r+i$	0.269	$<10^{-16}$	-0.18 ± 0.02	-0.07 ± 0.02	-0.42 ± 0.08	-0.54 ± 0.03	0.16 ± 0.01	
u	0.180	3.1×10^{-4}	-0.19 ± 0.04	-0.10 ± 0.04	0.20 ± 0.17		0.11 ± 0.03	
g	0.227	7.2×10^{-6}	-0.18 ± 0.04	-0.07 ± 0.04	0.28 ± 0.16		0.14 ± 0.03	
r	0.262	2.6×10^{-7}	-0.16 ± 0.04	-0.07 ± 0.04	0.04 ± 0.17		0.17 ± 0.03	hard
i	0.279	4.2×10^{-8}	-0.12 ± 0.04	-0.04 ± 0.04	-0.12 ± 0.17		0.18 ± 0.03	
$u+g+r+i$	0.237	$<10^{-16}$	-0.16 ± 0.02	-0.07 ± 0.02	-0.44 ± 0.09	-0.55 ± 0.04	0.15 ± 0.02	
u	0.229	1.3×10^{-7}	-0.20 ± 0.03	-0.09 ± 0.03	0.16 ± 0.14		0.14 ± 0.03	
g	0.270	4.6×10^{-10}	-0.18 ± 0.03	-0.07 ± 0.03	0.30 ± 0.14		0.16 ± 0.03	
r	0.280	1.0×10^{-10}	-0.18 ± 0.03	-0.08 ± 0.03	0.12 ± 0.14		0.17 ± 0.03	full
i	0.285	4.9×10^{-11}	-0.15 ± 0.03	-0.06 ± 0.03	-0.04 ± 0.14		0.18 ± 0.03	
$u+g+r+i$	0.266	$<10^{-16}$	-0.18 ± 0.02	-0.07 ± 0.02	-0.40 ± 0.08	-0.54 ± 0.03	0.16 ± 0.01	

Note. This table lists the best-fit multiple linear regression slopes of Equation (4) (for bands u, g, r, and i), and of Equation (7) (for $u+g+r+i$). Here r and rcc represent Spearman's correlation coefficient and significance level of the intrinsic correlation between $\sigma_{\rm rms}$ and $L_{\rm X}/L_{\rm bol}$ (controlling the effects of other parameters).

4.2. The Underlying Physics

Such a correlation appears consistent with the so-called X-ray reprocessing paradigm (Krolik et al. 1991), in which a variable central X-ray emission illuminates the accretion disk and produces variable reprocessed UV/optical radiation. Although the reprocessing paradigm can reproduce closely coordinated variations and lags between various bands, it faces severe challenges. The energy budget is one of the most prominent challenges as X-rays usually make up only a small fraction of the bolometric luminosity, and hence would be insufficient to drive strong enough UV/optical variation (e.g., Gaskell et al. 2007). Furthermore, the UV/optical inter-band lags observed are $\sim 3\times$ larger than the thin disk theory prediction (e.g., Fausnaugh et al. 2016; Jiang et al. 2017). The lag between UV and X-rays appears even up to $\sim$20 times larger the model prediction (McHardy et al. 2018). It was also found that UV/optical light curves are inconsistent with X-ray reprocessing in many sources, either showing too smooth variations or no clear correlation with X-rays (e.g., Maoz et al. 2002; Gaskell 2006; Gardner & Done 2017). Most recently, Zhu et al. (2018) pointed out that the reprocessing paradigm is unable to reproduce the observed timescale-dependent color variation observed in AGNs (Sun et al. 2014; Zhu et al. 2016), and this discrepancy cannot be reconciled under the general reprocessing paradigm. Considering all these challenges to the reprocessing mode, it is unlikely that the UV/optical variation in quasars is caused by X-ray reprocessing. Thus the intrinsic correlation between UV/optical variation and X-ray loudness in quasars does not necessarily support the reprocessing model.

As we noted earlier, $\sigma_{\rm rms}$ measures the $\sim$10 yr long variation amplitudes with a single parameter. To further probe the correlation between X-ray loudness and UV/optical variation at various timescales, we divide our quasar sample (with full band X-ray detection) equally into two subsamples according to their residual X-ray loudness to Equation (6), namely an X-ray-louder and X-ray-fainter sample. A Kolmogorov–Smirnov test confirms that the two subsamples have statistically indistinguishable distributions of redshift, black hole mass, bolometric luminosity, and Eddington ratio. Following di Clemente et al. (1996) and Zhu et al. (2016), we derive the ensemble structure function for each sample, i.e.,

$$\mathrm{SF}(\tau|\tau_{\rm min} < \tau < \tau_{\rm max}) = \sqrt{\frac{\pi}{2} < |m_i - m_j|>^2 - <\sigma_i^2 + \sigma_j^2>}, \quad (8)$$

where, for a given broad-band light curve, m_i and σ_i are the observed magnitude and error at epoch t_i, respectively, $\langle ... \rangle$ denotes averaging over all (m_i, m_j) or (σ_i, σ_j) observational pairs satisfying $\tau_{\rm min} < |t_i - t_j| < \tau_{\rm max}$, and the typical timescale τ is the logarithmic average between the minimal $\tau_{\rm min}$ and maximal $\tau_{\rm max}$ boundaries. Similarly, data points with photometric uncertainties greater than 0.2 mag are excluded. As the light curve of each quasar was similarly sampled in the observed frame, we present the ensemble structure functions as a function of timescale in the observed frame. Contrarily, using the rest frame would yield a biased structure function, e.g., with the data point at the longest rest frame timescale bin dominated by low-z sources.

The derived *ugri* structure functions are plotted in Figure 4, in which we can clearly see a stronger variation of the X-ray-louder sample, particularly at long timescales, consistent with the detection of an intrinsic correlation between X-ray loudness

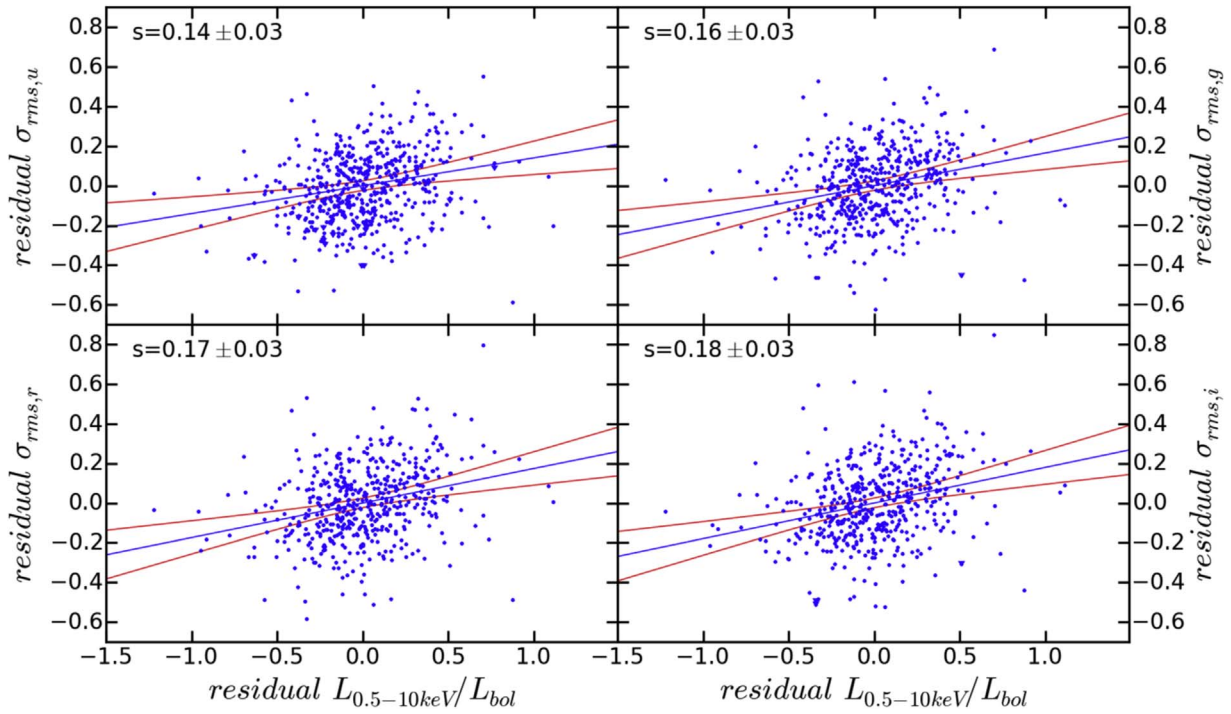

Figure 3. Residual *ugri* $\sigma_{\rm rms}$ to Equation (5) vs. the residual X-ray loudness to Equation (6). The scatter along the vertical axis is ∼0.2 dex, similar to that in Figure 1. Symbols and lines are the same as in Figure 1.

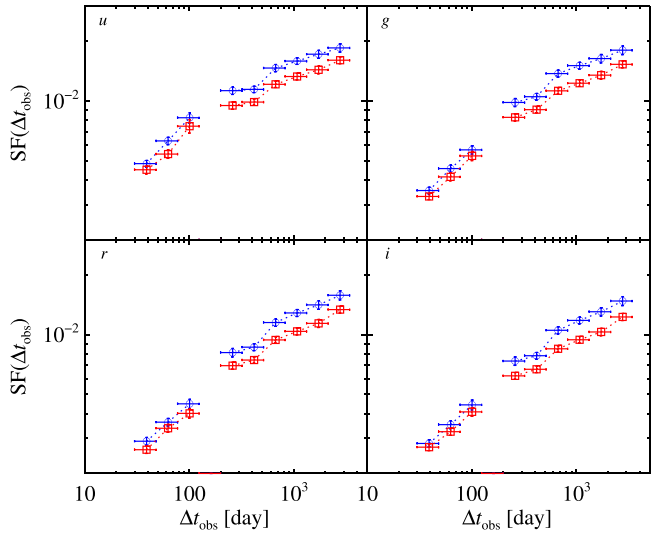

Figure 4. Comparison of the *ugri* ensemble structure function of quasars with relatively higher (blue) and lower (red) X-ray loudness. The errors in the structure function are derived through bootstrapping the samples. The gap around 200 days is due to the lack of timescale coverage of SDSS photometric observations.

and $\sigma_{\rm rms}$. It is interesting to note that the difference in structure function between two subsamples is gradually more prominent at longer timescales, and diminishes (or even disappears) at $\tau < 100$ days. This indicates that the physical link between X-ray loudness and UV/optical variation occurs on long timescales. This also disfavors the X-ray reprocessing paradigm in which a fast physical link is involved (the photon travel time from the central X-ray source to the UV/optical emitting accretion disc is a couple of days to weeks for quasars).

Instead, observations have shown that quasar variations, with characteristic timescales consistent with disk orbital or thermal timescales, can be attributed to disk thermal fluctuations driven by magnetic turbulence (Kelly et al. 2009). Inhomogeneous disk models accounting for such fluctuations appear well consistent with observations. The original model proposed by Dexter & Agol (2011) is able to match the disk size with microlensing observations, but this is larger than thin disk theory prediction. More excitingly, the revised inhomogeneous disk models by Cai et al. (2016, 2018) can further explain the observed timescale-dependent color variations and inter-band coordinations/lags without light echoing.

The intrinsic correlation between UV/optical variation and X-ray loudness discovered in this work thus indicates that, for quasars with stronger disk turbulence, more energy can be dissipated into the corona to produce X-ray emission. This can be naturally interpreted under the scenario that the X-ray corona in AGNs is heated through magnetic reconnection which is also associated with magnetic turbulence. The turbulence propagation along the disc (either inward, outward, or both) would be able to link the inner coronal heating to outer disc slow turbulence. The propagation takes a much longer time compared with X-ray reprocessing; however, its exact mechanism is as yet unclear. For instance, the pressure timescales for quasars could be decades to centuries, but the detection of changing-look quasars suggests the propagation may be on a timescale of 1–10 yr, similar to the timescale considered here. Note that the upper hot layer of the disc (where the sound speed could be much larger) and the ultra-fast disc outflow may also play a role in the propagation (Cai et al. 2018). Nevertheless, such long-term processes (compared with reprocessing) could naturally explain the fact that the intrinsic link between X-ray loudness and UV/optical variation is gradually stronger at longer timescales (Figure 4). We note that, even if the process occurs on longer timescales than observed, it may still yield an intrinsic correlation with a sufficiently large sample, and such an effect may also

contribute to the scatter in the correlation between X-ray loudness and UV/optical variation.

The multiple linear regression yields $\sigma_{\rm rms} \sim (L_{\rm X}/L_{\rm bol})^{\sim 0.16}$ (controlling the effects of other physical parameters). Analyzing using $\sigma_{\rm rms}$ as the independent variable and $L_{\rm X}/L_{\rm bol}$ as a dependent variable yields $L_{\rm X}/L_{\rm bol} \sim (\sigma_{\rm rms})^{\sim 0.43}$. A bisector slope for the correlation between $\sigma_{\rm rms}$ and $L_{\rm X}/L_{\rm bol}$ is ∼0.78, suggesting a close-to-linear intrinsic relation between them. It is interesting to note that the intrinsic correlation between $\sigma_{\rm rms}$ and X-ray loudness appears slightly stronger at longer wavelengths (see Table 1). This might be due to variation of dust attenuation along the line of sight to some quasars, which would produce flux variations in additional to the intrinsic one, mainly at shorter wavelengths. We also note that the intrinsic correlation between $\sigma_{\rm rms}$ and hard-band X-ray loudness is weaker compared with soft and full band. This is mainly because the hard X-ray sample is considerably smaller than the soft and full band samples. We build a sample with both soft and hard X-ray detections and find no obvious difference in the intrinsic correlation. We do not find a significant intrinsic correlation between $\sigma_{\rm rms}$ and X-ray hardness ratio either.

Various studies have detected a clear anticorrelation between X-ray loudness and luminosity/Eddington ratio of AGNs, indicating that highly accreting sources dissipate relatively less energy in the corona (e.g., Vasudevan & Fabian 2009; Lusso et al. 2010, 2012; Fanali et al. 2013). It is a fundamental question to understand what process controls the fraction of energy dissipated into the corona. The discovery in this work reveals that turbulence is (one of) the driving factor(s) behind these correlations.

We thank the anonymous referee for constructive suggestions that helped to improve the manuscript. This work is supported by National Basic Research Program of China (973 program, grant No. 2015CB857005) and National Science Foundation of China (grants No. 11421303 & 11503024). J.X.W. thanks support from Chinese Top-notch Young Talents Program, and CAS Frontier Science Key Research Program (QYZDJ-SSW-SLH006). Z.Y.C. acknowledges support from the China Postdoctoral Science Foundation (grant No. 2014M560515) and the Fundamental Research Funds for the Central Universities.

ORCID iDs

Wen-yong Kang https://orcid.org/0000-0003-2573-8100
Jun-Xian Wang https://orcid.org/0000-0002-4419-6434
Zhen-Yi Cai https://orcid.org/0000-0002-4223-2198
Fei-Fan Zhu https://orcid.org/0000-0002-5712-2370
Xin-Wu Cao https://orcid.org/0000-0002-2355-3498
Wei-Min Gu https://orcid.org/0000-0003-3137-1851
Feng Yuan https://orcid.org/0000-0003-3564-6437

References

Ai, Y., Yuan, W., Zhou, H., et al. 2010, ApJL, 716, L31
Ananna, T. T., Salvato, M., LaMassa, S., et al. 2017, ApJ, 850, 66
Bauer, A., Baltay, C., Coppi, P., et al. 2009, ApJ, 696, 1241
Cai, Z.-Y., Wang, J.-X., Gu, W.-M., et al. 2016, ApJ, 826, 7
Cai, Z.-Y., Wang, J.-X., Zhu, F.-F., et al. 2018, ApJ, 855, 117
Coatman, L., Hewett, P. C., Banerji, M., et al. 2017, MNRAS, 465, 2120
Coatman, L., Hewett, P. C., Banerji, M., & Richards, G. T. 2016, MNRAS, 461, 647
Dexter, J., & Agol, E. 2011, ApJL, 727, L24
di Clemente, A., Giallongo, E., Natali, G., Trevese, D., & Vagnetti, F. 1996, ApJ, 463, 466
Di Matteo, T. 1998, MNRAS, 299, L15
Fanali, R., Caccianiga, A., Severgnini, P., et al. 2013, MNRAS, 433, 648
Fausnaugh, M. M., Denney, K. D., Barth, A. J., et al. 2016, ApJ, 821, 56
Galeev, A. A., Rosner, R., & Vaiana, G. S. 1979, ApJ, 229, 318
Gardner, E., & Done, C. 2017, MNRAS, 470, 3591
Gaskell, C. M. 2006, in ASP Conf. Ser. 360, AGN Variability from X-Rays to Radio Waves, ed. C. M. Gaskell et al. (San Francisco, CA: ASP), 111
Gaskell, C. M., Klimek, E. S., & Nazarova, L. S. 2007, ApJ, submitted (arXiv:0711.1025)
Guo, H., Wang, J., Cai, Z., & Sun, M. 2017, ApJ, 847, 132
Jiang, Y.-F., Green, P. J., Greene, J. E., et al. 2017, ApJ, 836, 186
Kelly, B. C., Bechtold, J., & Siemiginowska, A. 2009, ApJ, 698, 895
Kozłowski, S. 2016, ApJ, 826, 118
Kozłowski, S. 2017, A&A, 597, A128
Kozłowski, S., Kochanek, C. S., Udalski, A., et al. 2010, ApJ, 708, 927
Krolik, J. H., Horne, K., Kallman, T. R., et al. 1991, ApJ, 371, 541
LaMassa, S. M., Urry, C. M., Cappelluti, N., et al. 2016, ApJ, 817, 172
Lusso, E., Comastri, A., Simmons, B. D., et al. 2012, MNRAS, 425, 623
Lusso, E., Comastri, A., Vignali, C., et al. 2010, A&A, 512, A34
MacLeod, C. L., Ivezić, Ž., Kochanek, C. S., et al. 2010, ApJ, 721, 1014
MacLeod, C. L., Ivezić, Ž., Sesar, B., et al. 2012, ApJ, 753, 106
Maoz, D., Markowitz, A., Edelson, R., & Nandra, K. 2002, AJ, 124, 1988
McHardy, I., Connolly, S., Cackett, K. E., et al. 2018, MNRAS, 480, 2881
Meusinger, H., Hinze, A., & de Hoon, A. 2011, A&A, 525, A37
Meusinger, H., & Weiss, V. 2013, A&A, 560, A104
Richards, G. T., Lacy, M., Storrie-Lombardi, L. J., et al. 2006, ApJS, 166, 470
Sesar, B., Ivezić, Ž., Lupton, R. H., et al. 2007, AJ, 134, 2236
Shen, Y., Richards, G. T., Strauss, M. A., et al. 2011, ApJS, 194, 45
Sun, M.-Y., Xue, Y.-Q., Wang, J.-X., Cai, Z.-Y., & Guo, H.-X. 2018, ApJ, 866, 74
Sun, Y.-H., Wang, J.-X., Chen, X.-Y., & Zheng, Z.-Y. 2014, ApJ, 792, 54
Vanden Berk, D. E., Wilhite, B. C., Kron, R. G., et al. 2004, ApJ, 601, 692
Vasudevan, R. V., & Fabian, A. C. 2009, MNRAS, 392, 1124
Vaughan, S., Edelson, R., Warwick, R. S., & Uttley, P. 2003, MNRAS, 345, 1271
Wilhite, B. C., Brunner, R. J., Grier, C. J., Schneider, D. P., & vanden Berk, D. E. 2008, MNRAS, 383, 1232
Wilhite, B. C., Vanden Berk, D. E., Kron, R. G., et al. 2005, ApJ, 633, 638
Wold, M., Brotherton, M. S., & Shang, Z. 2007, MNRAS, 375, 989
Zhu, F.-F., Wang, J.-X., Cai, Z.-Y., et al. 2018, ApJ, 860, 29
Zhu, F.-F., Wang, J.-X., Cai, Z.-Y., & Sun, Y.-H. 2016, ApJ, 832, 75
Zu, Y., Kochanek, C. S., Kozłowski, S., & Udalski, A. 2013, ApJ, 765, 106
Zuo, W., Wu, X.-B., Liu, Y.-Q., & Jiao, C.-L. 2012, ApJ, 758, 104

The Astrophysical Journal, 888:129 (2pp), 2020 January 10 https://doi.org/10.3847/1538-4357/ab63d1

Erratum: "An Intrinsic Link between Long-term UV/Optical Variations and X-Ray Loudness in Quasars" (2018, ApJ, 868, 58)

Wen-yong Kang[1,2], Jun-Xian Wang[1,2], Zhen-Yi Cai[1,2], Heng-Xiao Guo[3], Fei-Fan Zhu[1,2], Xin-Wu Cao[4,5,6], Wei-Min Gu[6,7], and Feng Yuan[4,6]

[1] CAS Key Laboratory for Research in Galaxies and Cosmology, Department of Astronomy, University of Science and Technology of China, Hefei 230026, People's Republic of China; kwy0719@mail.ustc.edu.cn, jxw@ustc.edu.cn, zcai@ustc.edu.cn
[2] School of Astronomy and Space Science, University of Science and Technology of China, Hefei 230026, People's Republic of China
[3] Department of Astronomy, University of Illinois at Urbana-Champaign, Urbana, IL 61801, USA
[4] Shanghai Astronomical Observatory, Chinese Academy of Sciences, 80 Nandan Road, Shanghai 200030, People's Republic of China
[5] Key Laboratory of Radio Astronomy, Chinese Academy of Sciences, Nanjing 210008, People's Republic of China
[6] SHAO-XMU Joint Center for Astrophysics, Xiamen University, Xiamen, Fujian 361005, People's Republic of China
[7] Department of Astronomy, Xiamen University, Xiamen, Fujian 361005, People's Republic of China
Received 2019 December 16; published 2020 January 16

1. Introduction

In the published paper of Kang et al. (2018), the absolute value of the ordinate in Figure 4 has not been correctly presented, owing to a careless error in our codes. We thank Yun-Jing Wu for pointing out this error when using our codes.

The revised Figure 4 is presented here. The major difference between the revised and the original figure is the absolute value of the *y*-axis. We also add a unit (mag) to the *y*-axis.

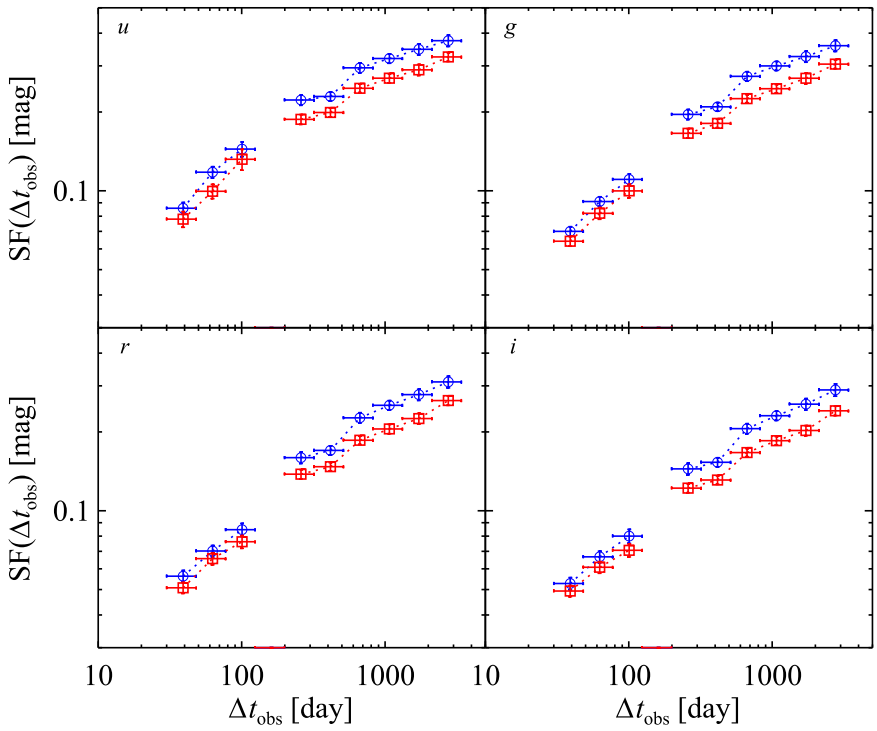

Figure 4. Comparison of the *ugri* ensemble structure function of quasars with relatively higher (blue) and lower (red) X-ray loudness. The errors in the structure function are derived through bootstrapping the samples. The gap around 200 days is due to the lack of timescale coverage of SDSS photometric observations.

These changes do not affect any of the scientific conclusions presented in Kang et al. (2018), as the figure was merely utilized to present the relative difference between the structure functions of two samples.

ORCID iDs

Wen-yong Kang https://orcid.org/0000-0003-2573-8100
Jun-Xian Wang https://orcid.org/0000-0002-4419-6434
Zhen-Yi Cai https://orcid.org/0000-0002-4223-2198
Fei-Fan Zhu https://orcid.org/0000-0002-5712-2370
Xin-Wu Cao https://orcid.org/0000-0002-2355-3498
Wei-Min Gu https://orcid.org/0000-0003-3137-1851
Feng Yuan https://orcid.org/0000-0003-3564-6437

Reference

Kang, W.-Y., Wang, J.-X., Cai, Z.-Y., et al. 2018, ApJ, 868, 58